

Tritium Labeling of Neuromedin S by Conjugation with [³H]N-Succinimidyl Propionate

Martin R. Edelmann,* Johannes Erny, Wolfgang Guba, and Markus Hierl



Cite This: *ACS Omega* 2023, 8, 2367–2376



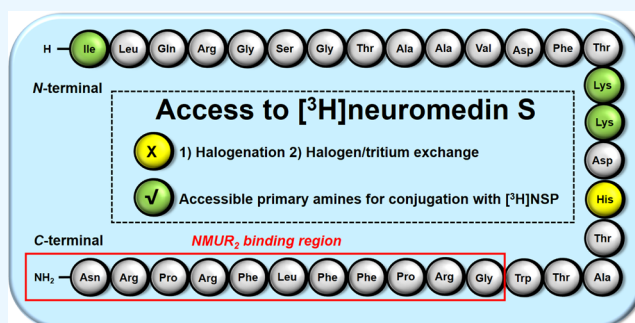
Read Online

ACCESS |

Metrics & More

Article Recommendations

ABSTRACT: The human neuropeptide neuromedin S (NMS) consists of 33 amino acids. The introduction of tritium atoms into NMS has not been described so far. This represents a gap for using [³H]NMS in radioreceptor binding assays or in tracking and monitoring their metabolic pathway. Two approaches for the incorporation of tritium into NMS were explored in this study: (1) halogenation at the His-18 residue followed by catalyzed iodine-127/tritium exchange and (2) conjugation of tritiated N-succinimidyl-[2,3-³H₃]propionate ([³H]NSP) to at least one of the three available primary amines of amino acids Ile-1, Lys-15, and Lys-16 in the peptide sequence. Although iodination of histidine was achieved, subsequent iodine-127/deuterium exchange was unsuccessful. Derivatization at the three possible amino positions in the peptide using nonradioactive NSP resulted in a mixture of unconjugated NSM and 1- to 3-conjugations at different amino acids in the peptide sequence. Each labeling position in the mixture was assigned following detailed LC–MS/MS analysis. After separating the mixture, it was shown in an *in vitro* fluorometric imaging plate reader (FLIPR) and in a competitive binding assay that the propionyl-modified NMS derivatives were comparable to the unlabeled NMS, regardless of the degree of labeling and the labeling position(s). A molecular simulation with NMS in the binding pocket of the protein neuromedin U receptor 2 (NMUR₂) confirmed that the possible labeling positions are located outside the binding region of NMUR₂. Tritium labeling was achieved at the N-terminal Ile-1 using [³H]NSP in 7% yield with a radiochemical purity of >95% and a molar activity of 90 Ci/mmol. This approach provides access to tritiated NMS and enables new investigations to characterize NMS or corresponding NMS ligands.



INTRODUCTION

Human neuromedin S (NMS) is a 33-amino acid neuropeptide belonging to the tachykinin family. It has been identified in the brain as an endogenous ligand for the orphan G-protein-coupled receptor (GPCR) FM-4/TGR-1 and acts on the neuromedin U (NMU) receptor 2 (NMUR₂) in the regulation of body weight homeostasis.^{1–3} The “S” nomenclature derives from the fact that NMS is highly expressed in the suprachiasmatic nucleus (SCN) of the hypothalamus. NMS is structurally related to human NMU (25-mer), first described in 1985 and named for its ability to stimulate smooth muscle contraction in the uterus.⁴ NMS and NMU both share an identical C-terminal heptapeptide (FLFRPRN-NH₂) including the amidated asparagine at the C-terminus in different species (e.g., chicken, mouse, Chinese softshell turtle, spotted gar, and Nile tilapia),⁵ indicating the importance of this peptide segment for receptor recognition. It was shown that this heptapeptide and the amidated asparagine are closely related to binding activity.^{6,7}

Radioisotope labeling of peptides is an essential tool to determine fate in *in vitro* and *in vivo* experiments. As all peptides contain hydrogen and carbon, the corresponding

radioisotopes are the most commonly used in biological studies. Tritium as a low-energy (18.6 keV) beta emitter has gained importance mainly because its half-life (12.3 years) is relatively long and the compounds can reach a high specific activity. However, the introduction of a tritium atom into a peptide is not straightforward. The incorporation of a tritiated amino acid into a peptide sequence is theoretically possible, but in practice, it is difficult and time-consuming when larger peptides are to be labeled. Catalytic titration is often complicated by the presence of interfering functional groups (e.g., thiol) within the peptide sequence, which can deactivate the catalyst during a reduction or exchange reaction. While tritium labeling has been reported for numerous neuropeptides, such as neuromedin N (6-mer),⁸ neuromedin U-8

Received: October 20, 2022

Accepted: December 7, 2022

Published: January 4, 2023



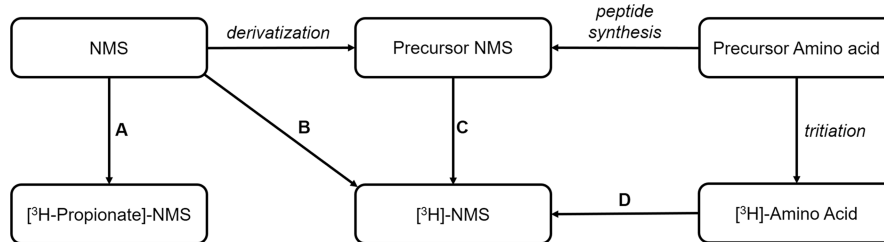


Figure 1. Considerations to tritium-labeled Neuromedin S (NMS). A: Derivatization of peptide using [^3H]N-succinimidyl propionate [^3H]NSP; B: catalytic hydrogen/tritium exchange starting from the native peptide; C: tritiation of the NMS precursor; D: peptide synthesis using tritiated amino acid.

(8-mer),⁹ angiotensin II (8-mer), and neurotensin 8–13 (6-mer),¹⁰ no tritium labeling concept for NMS has been published to date.

CONSIDERATIONS FOR TRITIATING PEPTIDES

Tritium labeling chemistry is often simple, and labeling can usually be performed late in the synthesis. The most stable labeling position is found in a carbon–tritium bond. There are various considerations for the introduction of a tritium atom into NMS, which are illustrated in Figure 1 and divided into four main routes: (A) derivatization with a tritium-labeled conjugate; (B) catalytic hydrogen/tritium exchange (HTE) starting from the native NMS; (C) tritiation of the NMS precursor. (D) solid-phase NMS synthesis using tritiated amino acid.

Late-stage tritium labeling by catalyzed HTE finds wide application in small molecules.^{11–13} These methods can only be applied to a limited extent for peptides. Promising approaches have been described, such as photoredox catalytic HTE in the peptide backbone.¹⁴ As this exchange is based on a radical mechanism, the consequence is the loss of existing chiral stereocenters in the peptide backbone. Another approach to late-stage labeling of peptides is the high-temperature solid-state catalytic isotope exchange reaction (HSCIE) described by Zolotarev and co-workers.¹⁵ HTE mainly occurs in the aromatic part of tyrosine residues, with an exchange at the *ortho*-position to the OH group. For small peptides, there is the possibility of total synthesis using tritiated amino acids as starting materials, either by solid-phase synthesis¹⁶ or by enzymatic couplings.¹⁷ The advantage is that the labeling position is known using characterized amino acids, and the specific activity can be adjusted as desired depending on the use of several ^3H -amino acids.

An alternative strategy for the synthesis of tritiated peptides is to use an appropriate peptide precursor. Access to peptide precursors can be achieved either by peptide synthesis using modified amino acids or by postmodification of the native peptide. Halogenated aromatic amino acids or amino acids containing double or triple bonds are widely used in peptide synthesis to design peptide precursors. Subsequent metal-catalyzed halogen/tritium exchange¹⁸ or reduction of the double/triple bond¹⁹ with tritium gas leads to the desired ^3H -peptide. Derivatization of a native peptide by direct iodination with nonradioactive iodine (^{127}I) using sodium iodide and an oxidizing agent, such as iodogen or chloramine-T, also leads to a peptide precursor. This results in iodination primarily at tyrosine residues but also at histidine residues in the sequence. Recently, the direct photochemical halogenation of peptides in a direct irradiation device and the single-pulse irradiation capillary reactor has been reported.²⁰ The specific halogenation

occurs with bromination at tyrosine, histidine, and tryptophan residues as well as with iodination at tyrosine and histidine residues. The halogens can subsequently be exchanged for tritium with tritium gas under metal catalysis.⁸

Another approach for tritiated peptides, especially larger peptides, is derivatization with a relatively small tritiated group. In analogy to protein derivatization,^{21,22} peptides can be tritiated by conjugation with the electrophilic *N*-succinimidyl-[2,3- $^3\text{H}_3$]propionate ([^3H]NSP). [^3H]NSP preferentially reacts with primary amines such as the *N*-terminal amine or with lysine residues.²³ Keller and co-workers were able to introduce amine functionality into peptides lacking lysines by modifying arginine residues with an amine linker and used this for conjugation with [^3H]NSP.¹⁰

RESULTS AND DISCUSSION

Preliminary Labeling Experiments on NMS: Preparation of the Iodinated Precursor. Commercially available NMS (human) has the following sequence: H-Ile-Leu-Gln-Arg-Gly-Ser-Gly-Thr-Ala-Ala-Val-Asp-Phe-Thr-Lys-Lys-Asp-His-Thr-Ala-Thr-Trp-Gly-Arg-Pro-Phe-Leu-Phe-Arg-Pro-Arg-Asn-NH₂. The synthesis of an NMS precursor was the first strategy explored. As described above in *Considerations for Tritiating Peptides*, derivatization with iodine-127 on Tyr is a common method for accessing peptide precursors. However, the peptide sequence of human NMS does not contain a Tyr but does contain a His residue. For this purpose, the reaction conditions of iodination at the His residue of NMS were optimized to synthesize an iodinated precursor. The peptide was treated at pH 5 and pH 10 with sodium iodide in four different oxidizing agents, namely, chloramine-T, Iodo-Beads (polymer-supported version of chloramine-T), iodogen, and the recently described chloramine oxidant.²⁴ The highest iodine incorporation was obtained using chloramine-T at pH 10 with 35% $^{127}\text{I}_1$ and 65% $^{127}\text{I}_2$ (Table 1).

Table 1. Iodine-127 Incorporation in NMS Dependent on pH and Oxidation Agent after 1 h, Analyzed by Mass Spectrometry

#	oxidation agent	pH	$^{127}\text{I}_0$ [%]	$^{127}\text{I}_1$ [%]	$^{127}\text{I}_2$ [%]
1	chloramine-T	5	35	56	9
2	chloramine-T	10	0	35	65
3	Iodo-Beads	5	76	24	0
4	Iodo-Beads	10	57	23	20
5	iodogen	5	90	10	0
6	iodogen	10	54	25	21
7	chloramine	5	93	7	0
8	chloramine	10	86	14	0

The catalytic exchange of iodine-127 to tritium is described in the literature exclusively on iodinated Tyr residues, although for the tritium labeling approach of peptides, direct iodination on His is also mentioned.²⁵ Therefore, the conditions were adopted in analogy to the iodine-127/tritium exchange on Tyr to tritiate the NMS precursor.²⁶ The iodinated precursor #2 (chloramine-T, pH 10) was selected for the exchange experiments, as it yielded the highest iodine-127 incorporation in His. PdO/BaSO₄ (10% Pd) and Pd/C (10% Pd) were tested as catalysts for an ¹²⁷I-His deuterium exchange in dimethylformamide as the solvent. As a further variation, the experiments were each carried out with and without the addition of 1 μ L of triethylamine in the presence of deuterium gas at 22 °C for 2 h. However, a successful exchange was not achieved at the deuterium manifold in any of the experiments. As the reaction optimization was too time-consuming in this case, the approach of tritium labeling of NMS by means of oxidative iodination followed by reductive tritium dehalogenation was discontinued. An alternative to an iodine-127/tritium exchange at His would be a halogen (bromo or iodo) tritium exchange at Phe using a halogenated precursor. As the peptide does not consist of any sulfur-containing amino acids that could affect catalysis, this would be a promising concept. However, the synthesis of a suitable halogen precursor was not considered in this study.

Preliminary Labeling Experiments on NMS: Derivatization Using NSP. The feasibility of derivatization on amine residues was investigated. NMS consists of three primary amines that can be tagged with NSP: Ile-1, Lys-15, and Lys-16. Compared to the size of NMS (3790 Da), derivatization from a small [³H₃]propionate (62 Da) contributes only a marginal difference in mass. However, the derivatization changes the molecular structure and this could lead to altered biological or physicochemical behavior. For this reason, the corresponding nonradioactive NSP was specifically placed at different positions of the peptide and these derivatives were subsequently investigated for their functionality and binding behavior toward NMUR₂. In a first preliminary experiment, NMS was treated in an equimolar ratio with NSP in PBS at pH 8.5 for 30 min at 22 °C. Following the 1:1 reaction, theoretically, a maximum of eight NMS derivatives with a modification at the following amino acids can be present: (1) unlabeled; (2) Ile-1; (3) Lys-15; (4) Lys-16; (5) Ile-1 + Lys-15; (6) Ile-1 + Lys-16; (7) Lys-15 + Lys-16; (8) Ile-1 + Lys-15 + Lys-16. However, HPLC analysis of the crude reaction mixture showed seven peaks (Figure 2). Five fractions were isolated from the preparative HPLC, with fractions “b” and “d” each consisting of two nonseparable products.

In the next preliminary experiment, NMS was treated with 3 equiv of NSP under identical reaction conditions to the equimolar approach. The main product from the crude reaction solution was assigned to peak e. Furthermore, the peptide derivatives related to the peaks d₁ and d₂ were found in the reaction mixture. Finally, an excess of 3 equiv of NMS was treated with NSP. Analytical HPLC showed that the major component in the reaction solution after 30 min was the unlabeled peptide as expected, but fractions b₁, b₂, and c were also detected. It was shown in the preliminary experiments that when treating NMS with different molar ratios of NSP, the distribution of the products formed can be controlled. The next steps are to identify the labeling positions of fractions a–e and to determine which labeling position has the least

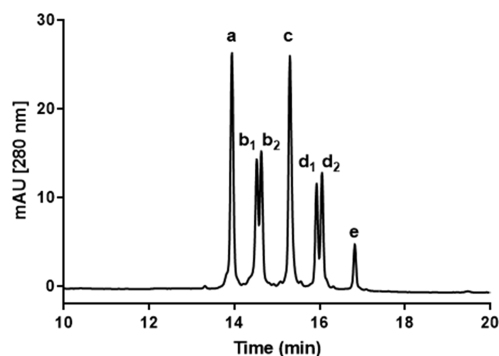


Figure 2. HPLC analysis of the crude solution on NMS treated with 1 equiv of NSP showed seven peaks with retention times between 14 and 17 min. Assignment of a–e refers to the isolated fractions, where b and d consist of two nonseparable products.

influence on the biological behavior compared to the unlabeled peptide.

Identification of Labeling Position Using LC-ESI-MS/MS. From the five isolated fractions a–e of the preparative purification from the equimolar labeling experiment with nonradioactive NSP, the labeling positions were identified by LC-ESI-MS/MS. In this process, a separation of the mixed fractions b and d was achieved, which ensured an investigation of the main peaks from the mass trace of the total ion chromatogram (TIC) (Figure 3).

Each spectrum below the low-energy MS trace was summed up and deconvoluted. The resulting mass spectra (Figure 4) showed the monoisotopic mass ($[M + H]^+$) of the intact peptides from fractions a–e and indicated the number of labeled amino acids of the peptide. In the case of unlabeled NMS, the calculated $[M + H]^+$ is 3790.0206 Da. For each labeling event that would take place, the calculated mass increases by +56.0262 Da. From these intact masses, it can be concluded how often the activated propionic acid was conjugated to the three possible positions of the peptide.

Table 2 shows the theoretical masses of NMS containing 0 to 3 labels of propionate as well as the found masses of the intact peptides. The masses of fractions a–e were assigned as follows: Unlabeled NMS has been found in fraction a. Fraction b consisted of two peaks (b₁ and b₂), and fraction c gave a mass suggestive of a single label. In each of the two peaks of fraction d (d₁ and d₂), a double labeling event of NSP was detected. In fraction e, a mass increase of three labels was found, indicating that conjugation occurred at all three possible positions of the primary amines present in the peptide.

Although it is possible to determine the number of labels from the masses of intact peptides from the low-energy trace, it is not possible to obtain information about the exact label position. To determine the exact positions of the propionyl labels from fractions a–e, a peptide mapping was carried out. The most common peptide fragments observed in high-energy collisions are b ions and y ions.²⁷ The b ions appear to extend from the N-terminus, while the y ions appear to extend from the C-terminus. The mass pattern in the high-energy trace has shown a more prominent y ion series (compared to the b ion series) in the mid-mass and high mass ranges (Figure 5).

As already mentioned, the mass from fraction a correlates with the unlabeled NMS. In fraction b, which consists of two peaks, it was shown in b₁ that the mass shift occurred in the y₁₉ ion, which corresponds to Lys-15 from the peptide sequence.

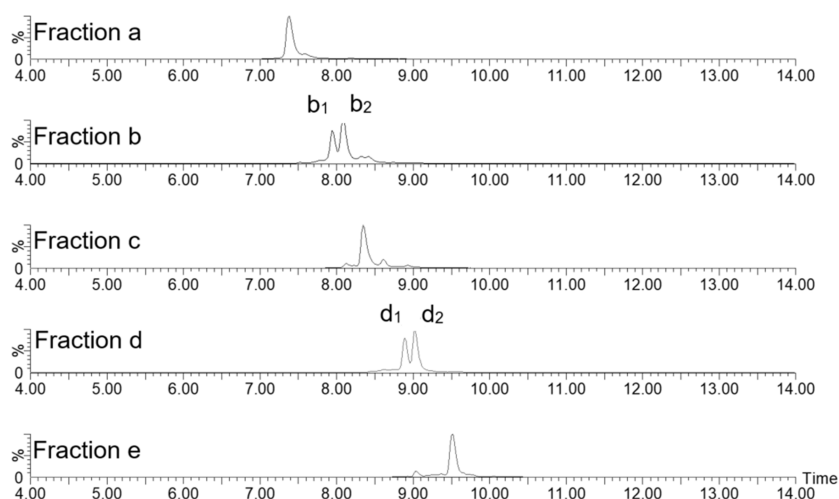


Figure 3. LC/MS chromatograms (MS trace; TIC: 100–2000 Da) of the fractions a–e.

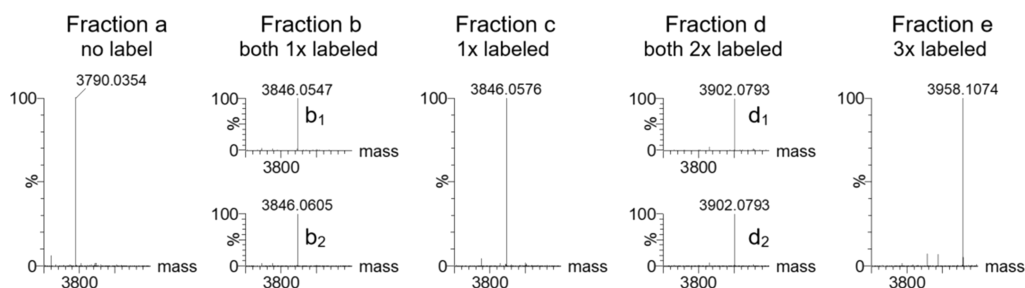


Figure 4. Deconvoluted low-energy mass ($[M + H]^+$) spectra of the main peaks of the fractions a–e.

Table 2. Found Masses underneath Chromatographic Peaks in Low-Energy Trace

fraction/ peak	retention time [min]	found mass [Da]	assignment	theoretical mass [Da]	mass error [ppm]
a	7.4	3790.0354	NMS	3790.0206	3.9
b ₁	7.9	3846.0547	1× labeled NMS	3846.0468	2.1
b ₂	8.1	3846.0605	1× labeled NMS	3846.0468	3.6
c	8.3	3846.0576	1× labeled NMS	3846.0468	2.8
d ₁	8.9	3902.0793	2× labeled NMS	3902.0730	1.6
d ₂	9.0	3902.0793	2× labeled NMS	3902.0730	1.6
e	9.5	3958.1074	3× labeled NMS	3958.0992	2.1

In peak b₂, the mass shift happened in the y₁₈ ion, which represents a label on Lys-16. With respect to fraction c, in which the peptide was also singly labeled, there was no mass shift in y₁₈ and y₁₉, whereas a mass shift was observed in y₃₃. This shows that the labeling took place at the N-terminal amino acid Ile-1. In fraction d, which also consisted of two peaks and in which each showed a double labeling in the low-energy trace, both peaks were assigned. The y ions 19 and 33 from peak d₁ showed a mass shift, resulting in labeling at Ile-1 and Lys-15. For d₂, the shift was at y ions 18 and 33, resulting in labeling at Ile-1 and Lys-16. As already known, the peptide from fraction e was triply labeled and the mapping confirmed a mass shift at y₁₈, y₁₉, and y₃₃. Consequently, conjugation with NSP took place at amino acids Ile-1, Lys-15, and Lys-16. The

exact labeling positions in the peptide sequence were assigned to each fraction or peak, and they are listed in Table 3. However, one compound was not found: a double labeling of NMS on Lys-15 and Lys-16. This is surprising, as conjugation to both lysine residues was observed with the triple-labeled NMS. The labeling experiments also did not show which amine reacts first with NSP. This raises the question of whether the N-terminal Ile has an influence on the reactivity of the lysines or whether it is a sterically hindered effect.

Functional *In Vitro* Fluorometric Imaging Plate Reader Assay. To compare the functional activities of propionyl-modified and unlabeled NMS derivatives, an *in vitro* fluorometric imaging plate reader (FLIPR) assay was performed. The aim is to demonstrate whether the degree of labeling as well as the labeling position has an influence on the half maximal effect concentration (EC₅₀). The NMUR₂ FLIPR assay was run in homogeneous format in the 384-well format. All tested fractions are shown in Figure 6. Fraction b (pEC₅₀ = 8.75 ± 0.12), fraction c (pEC₅₀ = 8.99 ± 0.20), fraction d (pEC₅₀ = 9.01 ± 0.05), and fraction e (pEC₅₀ = 9.00 ± 0.12) all show similar activities compared to the unlabeled NMS (fraction a, pEC₅₀ = 9.11 ± 0.27), indicating that the modifications are not interfering with the binding and functional activity of the peptides at the receptor.

***In Vitro* Affinity Receptor Binding.** The results from the functional *in vitro* FLIPR assay were confirmed by a second assay. The affinities of unlabeled and propionyl-modified NMS with respect to specific binding to the human NMUR₂ receptor were compared in a competitive binding assay using ¹²⁵I-labeled NMU-8 (porcine).²⁸ The obtained dose–response curves are shown in Figure 7. The resulting IC₅₀ values as well

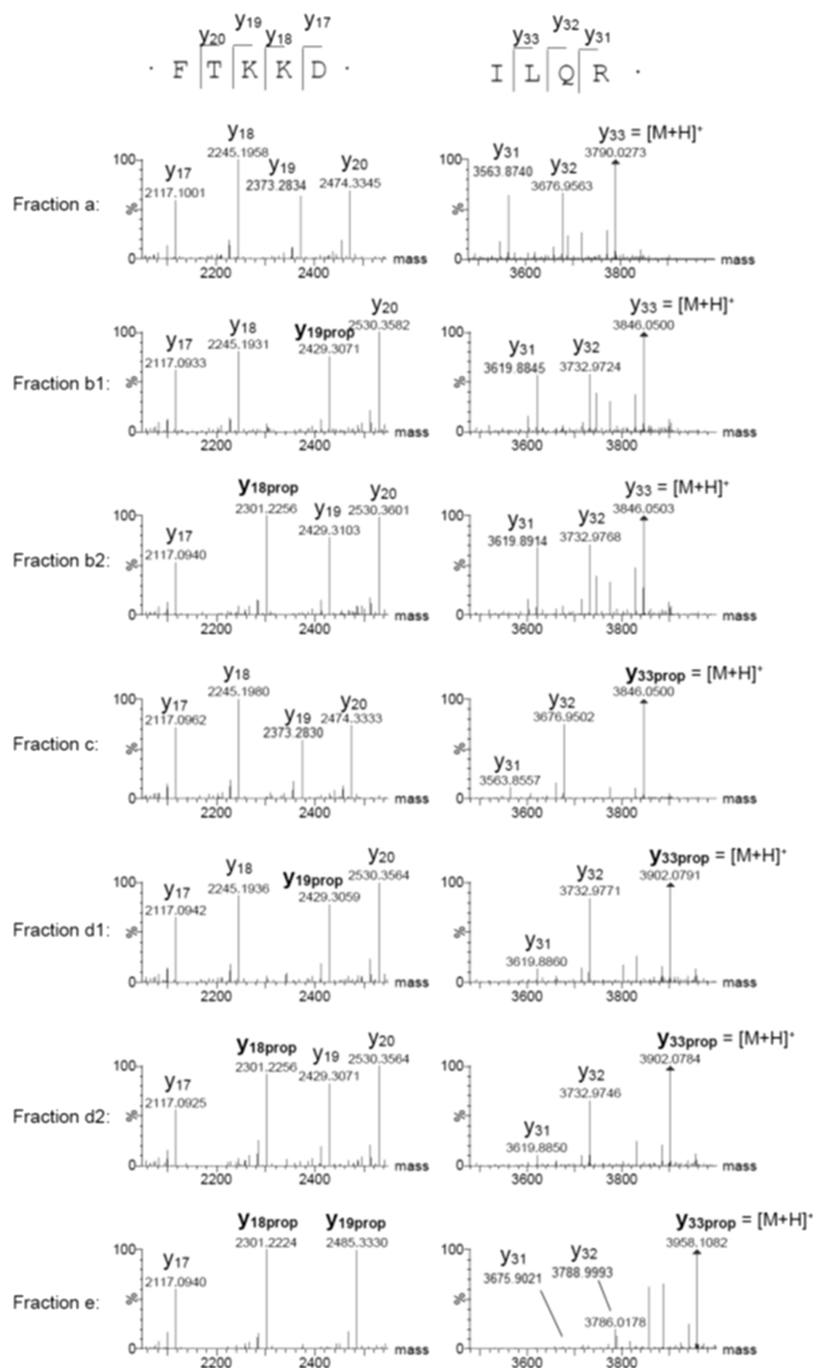


Figure 5. y ion pattern of high-energy MS spectra of fractions a–e. y ions marked with “prop” indicate the labeling positions. Zoom left column: 2050–2550 Da; zoom right column: 3480–4000 Da.

Table 3. Propionyl-Labeled Amino Acids of the Peptide Sequences from Fractions a–e Are Marked with “*” According to the High-Energy Trace Mass Spectrometry Analyses

fraction/peak	labeling position	peptide sequence
a	non	ILQRGSGTAAVDFTKKDHTATWGRPFLLFRPRN-NH ₂
b ₁	Lys-15	ILQRGSGTAAVDFTK*KDHTATWGRPFLLFRPRN-NH ₂
b ₂	Lys-16	ILQRGSGTAAVDFTKK*DHTATWGRPFLLFRPRN-NH ₂
c	Ile-1	I*LQRGSGTAAVDFTKKDHTATWGRPFLLFRPRN-NH ₂
d ₁	Ile-1, Lys-15	I*LQRGSGTAAVDFTK*KDHTATWGRPFLLFRPRN-NH ₂
d ₂	Ile-1, Lys-16	I*LQRGSGTAAVDFTKK*DHTATWGRPFLLFRPRN-NH ₂
e	Ile-1, Lys-15, Lys-16	I*LQRGSGTAAVDFTK*K*DHTATWGRPFLLFRPRN-NH ₂

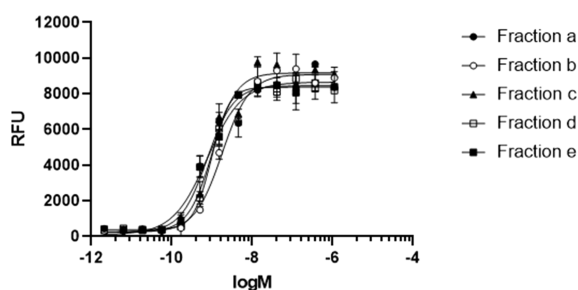


Figure 6. Concentration–response curves (CRCs) for fractions a–e in *in vitro* FLIPR assay. The *y*-axis represents the maximum minus baseline fluorescence signal for each sample. The *x*-axis represents the log of the molar concentration. Data were fitted by the Hill equation, and data points represent the mean \pm standard deviation of two individual experiments.

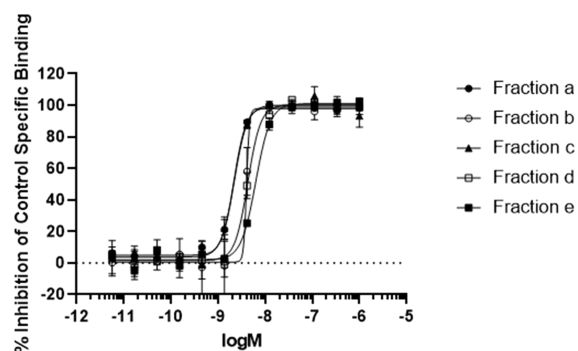


Figure 7. Concentration–response curves (CRCs) for fractions a–e in *in vitro* affinity receptor binding assay. The *y*-axis represents the percentage of inhibition of specific binding for the radiolabeled ligand [^{125}I]NMU-8 for each sample. The *x*-axis represents the log of the molar concentration. Data were fitted by the Hill equation, and data points represent the mean \pm standard deviation of two individual experiments.

as the calculated negative logarithms of the IC_{50} values (pIC_{50}) and the inhibition constants (K_i) of fractions a–e were similar (Table 4). It is noticeable that the unlabeled NMS (fraction a)

Table 4. IC_{50} , Calculated pIC_{50} , and K_i Values of Fractions a–e^a

compound/fraction	IC_{50} [M]	pIC_{50} [M]	K_i [M]
NMU-8	1.5×10^{-10}	9.82	1.2×10^{-10}
a	2.2×10^{-9}	8.66	1.8×10^{-9}
b	4.0×10^{-9}	8.39	3.3×10^{-9}
c	2.2×10^{-9}	8.66	1.8×10^{-9}
d	4.3×10^{-9}	8.37	3.5×10^{-9}
e	6.3×10^{-9}	8.20	5.2×10^{-9}

^aThe values are given as the mean value in molarity [M] of two independent experiments.

showed the identical IC_{50} value as the N-terminally single-labeled NMS derivative of fraction c, whereas the single labeling of one of the two Lys within the sequence (fraction b) showed a minor influence on the IC_{50} . In fraction d, in which there was double labeling of Ile-1 and one of the two Lys, the IC_{50} was almost identical to that of fraction b. This also suggests that labeling at the N-terminal amino acid Ile-1 has no influence on the inhibition concentration. The triple-labeled

NMS derivative from fraction e showed the highest influence on the IC_{50} value.

These results are in line with the data obtained from the functional *in vitro* FLIPR assay, in which all tested fractions also showed similar effects and no significant differences in their functional activities. A single label at the N-terminal Ile-1 seems to have no influence on the functionality as well as on binding to NMUR₂, suggesting that a modification at Ile-1 is preferred.

Molecular Dynamics Simulation. Jiang *et al.* recently published cryo-electron microscopy (cryoEM) structures of Gq chimera-coupled NMUR₁ and NMUR₂ together with bound human NMU-25 and NMS.²⁹ In the NMUR₂-NMS structure, only the final 11 C-terminal NMS amino acids Gly-23 to Asn-33 are visible (Figure 8). Of those residues, Gly-23 to Pro-25 are not engaged in interactions with the protein.

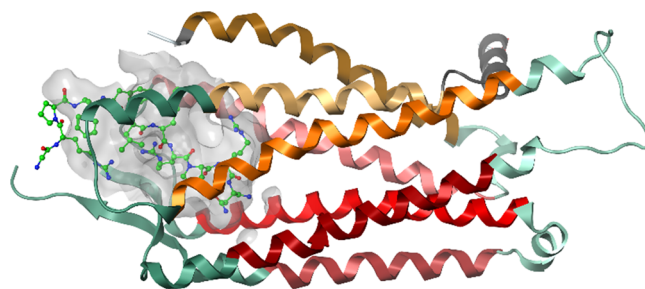


Figure 8. NMS in the binding pocket of NMUR₂ (PDB code 7W57). Phe-26 to Asn-33 are engaged in intermolecular interactions with the receptor.

As the labeling positions are obviously distant from the peptide-binding pocket, the derivatization with NSP is not expected to interfere with the binding of the peptide to the protein. This was indeed confirmed by FLIPR and receptor binding data with the modified peptides, which did not show an impact on functional activity. Therefore, it is reasonable to assume that the derivatized residues do not interact with the protein.

Tritium Labeling of NMS. Based on the results of the functional activity and competitive binding assay, as well as the confirmation from molecular dynamics simulation, a modification at the amine residue of Ile-1 has no influence on the binding of the derivatized NMS to the protein NMUR₂. Therefore, in analogy to the nonradioactive preliminary experiments, the conjugation was carried out with radioactive [^3H]NSP (1 equiv) and NMS (4 equiv). An HPLC analysis using a UV and radio detector of the crude solution (Figure 9A) showed, as expected, the unlabeled NMS as the major compound. Peak b showed a double peak in UV, corresponding to conjugation to Lys-15 and Lys-16, respectively, but there was no separation in the radio peak. Furthermore, the desired product of the N-terminal conjugation at Ile-1 was formed.

By means of preparative HPLC, peak b, as a mixture of b₁ and b₂, and peak c were isolated in high purity (Figure 9B,C). The radiochemical yields at b and c of 13% and 7%, respectively, indicate that a high amount of [^3H]NSP was hydrolyzed during the conjugation process. This was confirmed by a radioactivity measurement of the waste obtained from the dialysis of 50% of the initiated radioactive amount. On careful inspection of Figure 9C, a tailing can be

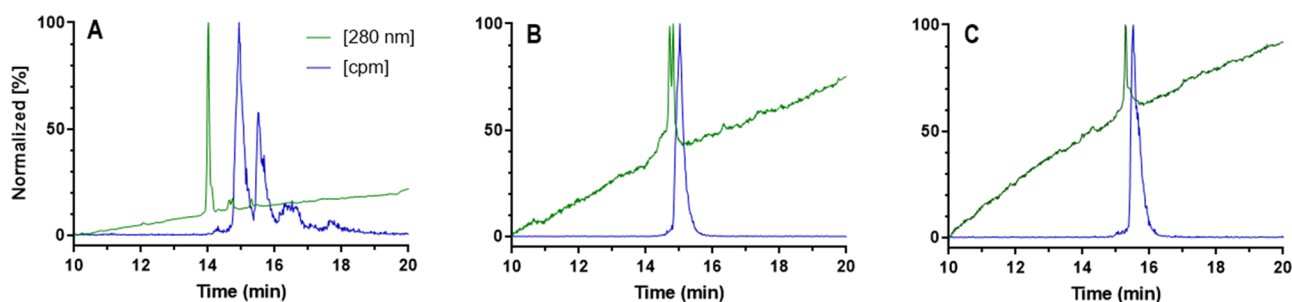


Figure 9. Analytical HPLC shows the normalized chromatograms of (A) crude solution after dialysis, (B) isolated fraction from peak B, and (C) isolated fraction C. Green lines: absorbances at the wavelength of 280 nm. Blue lines: time-shifted radio detection in counts per min (cpm).

found in the isolated peak c, especially in the radioactive detection. A similar tailing can also be found in the UV trace of the unlabeled NMS peak in Figure 9A. This tailing is probably due to the fact that in an analysis of the commercial NMS batch used for the radioactive conjugation, an impurity of about 8% (data not shown) of the corresponding C-terminal carboxylic acid is detected instead of the amide. This tailing is also seen in the non-radioactive NSP/NMS (3:1) preliminary experiment, as the identical batch was used here. In the equimolar preliminary experiment, which was the first conjugation experiment in this study, a different batch was used and in this case, the HPLC analysis shows no tailing. It is worthwhile to carefully analyze the commercially available starting material before radiolabeling.

CONCLUSIONS

Two approaches were investigated for the incorporation of tritium into human NMS: (1) halogenation of NMS followed by metal-catalyzed halogen/tritium exchange; (2) derivatization of primary amine residues using [^3H]NSP. Halogenation was achieved with sodium iodide and chloramine-T at His residues (0% $^{127}\text{I}_0$, 35% $^{127}\text{I}_1$, and 65% $^{127}\text{I}_2$), but subsequent exchange of iodine-127 to deuterium was unsuccessful. In a nonradioactive preliminary experiment, NSP was conjugated to primary amines available at the following amino acids in the peptide sequence: Ile-1, Lys-15, and Lys-16. In a functional *in vitro* FLIPR and competitive binding assay, it was demonstrated that the binding behavior between the modified NMS derivatives and the protein NMUR₂ is comparable to that of the unlabeled NMS, regardless of the degree of labeling and the labeling position, with the preferred labeling position at the N-terminal amino acid Ile-1. These results allowed conjugation with radioactive NSP to NMS. After preparative HPLC purification, two main fractions with radioactive peptide derivatives were isolated. The first fraction consisted of a mixture of a single conjugation at Lys-15 and another product with a label at Lys-16 (total yield: 13%), which was not separable due to the almost identical retention time. The second major fraction consisted of the desired conjugation product with a single label at the N-terminal Ile-1 (yield: 7%) in high purity (>95%) and a molar activity of 90 Ci/mmol. This study reports, to the best of our knowledge, the first approach to tritiated NMS, which opens the door for further studies to characterize and investigate NMS or corresponding ligands.

MATERIALS AND METHODS

All chemical starting materials are commercially available and have been used without further purification. Neuromedin S

(NMS) peptide (human) was purchased from Abbexa Ltd. (Cambridge, UK). Nonradioactive *N*-succinimidyl propionate (NSP) was obtained from FUJIFILM Wako (Osaka, Japan). Tritium-labeled [^3H]N-succinimidyl propionate ([^3H]NSP) (molar activity: 90 Ci/mmol) was obtained from Pharmaron (Cardiff, Wales, UK) as a solution in toluene (5 mCi/mL). Dulbecco's phosphate-buffered saline (PBS, Gibco, Paisley, UK) was adjusted with 1 M NaOH to pH 8.5. Liquid scintillation counting was accomplished using a HIDEX 300 SL and ULTIMATE GOLD cocktail (PerkinElmer Inc., Waltham, MA, USA). Analytical HPLC was performed using an Agilent 1210 series HPLC system (Santa Clara, CA, USA) using a Waters XBridge Phenyl column (4.6 mm \times 150 mm, 3.5 μm). HPLC conditions: mobile phase [A]: H₂O + 5% acetonitrile + 0.1% TFA (v/v/v), [B]: acetonitrile + 0.1% TFA (v/v), gradient 5% [B] to 65% [B] over 20 min with a flow rate of 1 mL/min. Radiochemical purity was measured using the β Radioactivity-HPLC flow detector RAMONA* (Elysia-raytest, Straubenhardt, Germany), combined with a RAMONA-HPLC-pump for continuous admixture of liquid-scintillator cocktail (flow rate: 2 mL/min) to the eluate of the HPLC system. Preparative purification was performed by the use of a Gilson PLC 2050 (Middleton, WI, USA), equipped with a Waters XBridge Phenyl column (300 mm \times 10 mm, 5 μm) under the following conditions: Solvent [A] was water + 5% acetonitrile + 0.1% trifluoroacetic acid (v/v/v) and solvent [B] was acetonitrile + 0.1% trifluoroacetic acid (v/v). The column was initially equilibrated at 5% [B] using a flow rate of 6 mL/min, with the absorbance monitored at 280 nm. Starting with isocratic conditions of 5% [B] for 2 min, a linear gradient to 65% [B] was followed over 38 min. Float-A-Lyzer Dialysis Devices were obtained from Thermo Fisher Scientific (Waltham, MA, USA), with volume sizes of 1 or 5 mL and a molecular weight cut-off of 500–1000 Da.

Direct Iodination of NMS. Direct iodination was investigated with four oxidizing agents at pH 5 and pH 10. NMS (0.5 mg, 0.13 μmol) was dissolved in 0.5 mL of PBS (pH 5 or pH 10) in a 1.5 mL LoBind Eppendorf tube. Fifty nine micrograms (0.40 μmol , 3 equiv) of sodium iodide, dissolved in 3.7 μL of PBS at pH 7.3, was added. Four equivalents (0.53 μmol) of oxidation agents chloramine-T (0.12 μg in 8.5 μL of PBS at pH 7.3), iodogen (0.23 μg in 11.8 μL of PBS at pH 7.3), and freshly prepared chloramine according to a published procedure²⁴ was added. When using polymer-bound chloramine-T (loading: 0.2 mmol/g), a single bead with a weight of 15 mg was used, which corresponds to an amount of substance of about 3 μmol (22.7 equiv). The eight samples were shaken at 22 $^\circ\text{C}$ by a horizontal rotation of 600 rpm. After 1 h, the

samples were analyzed for their incorporation of iodine by mass spectrometry.

Equimolar Treatment of NMS with NSP. NMS (4.5 mg, 1.19 μmol) was dissolved in 1 mL of PBS at pH 8.5 in a 5 mL LoBind Eppendorf tube to give a colorless solution. Two hundred three micrograms (1.19 μmol) of NSP, dissolved in 6.8 μL of DMSO, was added, and the solution was shaken orbitally at 22 $^{\circ}\text{C}$ for 30 min. The solution was diluted with 4 mL of water transferred into a 5 mL Float-A-Lyzer for solvent exchange into water. The water was exchanged three times after 30 min and stored in the fridge at 4 $^{\circ}\text{C}$ for 16 h. Analytical HPLC at 280 nm showed the following ratios of the peaks with the corresponding retention time in brackets: 33% a (14.0 min); 11% b₁ (14.6 min); 11% b₂ (14.7 min); 23% c (15.4 min); 8% d₁ (16.0 min); 10% d₂ (16.2 min); 4% e (16.9 min). The crude protein solution was lyophilized, and the residue was dissolved in 1 mL of water + 0.5% trifluoroacetic acid for preparative purification. The five fractions a–e (Figure 1) were separated as a colorless solid from the crude mixture and resulted in the following weights after lyophilization: a: 1.1 mg; b: 0.7 mg; c: 1.0 mg; d: 0.8 mg; e: 0.3 mg. The corresponding labeling positions are described in Results and Discussion. HRMS (ESI) calculated for fraction b₁: $[\text{M} + \text{H}]^+ \text{C}_{176}\text{H}_{270}\text{N}_{53}\text{O}_{46}^+$: 3846.0468 m/z ; found: 3846.0547 m/z ; calculated for fraction b₂: $[\text{M} + \text{H}]^+ \text{C}_{176}\text{H}_{270}\text{N}_{53}\text{O}_{46}^+$: 3846.0468 m/z ; found: 3846.0605 m/z ; calculated for fraction c: $[\text{M} + \text{H}]^+ \text{C}_{176}\text{H}_{270}\text{N}_{53}\text{O}_{46}^+$: 3846.0468 m/z ; found: 3846.0576 m/z ; calculated for fraction d₁: $[\text{M} + \text{H}]^+ \text{C}_{179}\text{H}_{274}\text{N}_{53}\text{O}_{46}^+$: 3902.0730 m/z ; found: 3902.0793 m/z ; calculated for fraction d₂: $[\text{M} + \text{H}]^+ \text{C}_{179}\text{H}_{274}\text{N}_{53}\text{O}_{46}^+$: 3902.0730 m/z ; found: 3902.0793 m/z ; calculated for fraction e: $[\text{M} + \text{H}]^+ \text{C}_{182}\text{H}_{278}\text{N}_{53}\text{O}_{47}^+$: 3958.0992 m/z , found: 3958.1074 m/z .

Treatment of NMS with Three-Fold Excess of NSP.

The conjugation of NMS with 3 equiv of NSP was carried out in analogy to the described equimolar procedure with the following amounts: 3.3 mg (0.88 μmol) of NMS in 1.5 mL of PBS at pH 8.5 in a 5 mL LoBind Eppendorf tube and 462 μg (2.70 μmol) of NSP, dissolved in 9.5 μL of DMSO. Analytical HPLC at 280 nm (Figure 10) showed the following ratios of

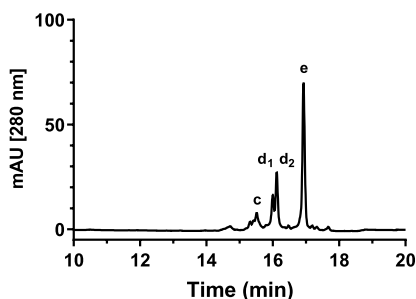


Figure 10. HPLC analysis of the crude solution on NMS treated with 3 equiv of NSP (for assignments of c–e, see the text).

the peaks with the corresponding retention time in brackets: 8% c (15.4 min); 12% d₁ (16.0 min); 20% d₂ (16.2 min); 61% e (16.9 min). After preparative purification and lyophilization, 2.2 mg (0.56 μmol ; yield: 64%) of the major peak e was isolated as a colorless solid with a purity of 97%.

Treatment of Three-Fold Excess of NMS with NSP.

The conjugation of 3 equiv of NMS with NSP was carried out in analogy to the described equimolar procedure with the

following amounts: 3.0 mg (0.79 μmol) of NMS in 1.5 mL of PBS at pH 8.5 in a 5 mL LoBind Eppendorf tube and 45 μg (0.26 μmol) of NSP, dissolved in 9.5 μL of DMSO. Analytical HPLC at 280 nm (Figure 11) showed the following ratios of

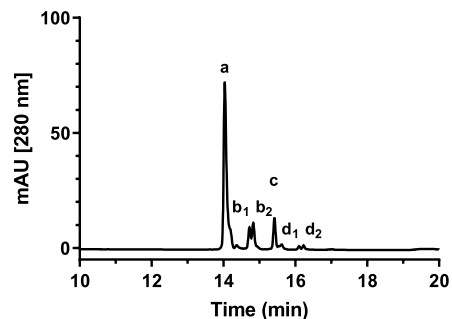


Figure 11. HPLC analysis of the crude solution on NMS:NSP (3:1) (for assignments of a–d, see the text).

the peaks with the corresponding retention time in brackets: 70% a (14.0 min); 7% b₁ (14.7 min); 9% b₂ (14.8 min); 11% c (15.4 min); 1% d₁ (16.1 min); 2% d₂ (16.2 min).

LC–MS/MS Analysis. LC-ESI-MS/MS was carried out on a Waters iClass HPLC system using a Waters UPLC BEH C18 column (1.0 mm \times 150 mm, 1.7 μm), and the column temperature was set to 40 $^{\circ}\text{C}$. Mobile phase [A]: H₂O + 0.1% formic acid (v/v); [B]: acetonitrile + 0.1% formic acid (v/v). Starting with isocratic conditions of 5% [B] for 1 min followed by the gradient 5% [B] to 40% [B] over 10 min and 40% [B] to 95% [B] over 6 min. The flow rate was set to 80 $\mu\text{L}/\text{min}$. Detection was performed first on a UV detector at 214 and 280 nm (TUV, Waters iClass) followed by a Synapt G2 HDMS QToF (Waters, Manchester, UK) equipped with an ESI source and adjusted with common voltages for MS peptide analysis. The collision energy for low-energy trace was switched off and ramped from 16 V up to 42 V for the high-energy trace. The data were acquired, processed, and analyzed in Waters MassLynx software.

Functional In Vitro FLIPR Assay. Recombinant Chem-1 cells overexpressing the full-length human NMUR₂ were cultured at 37 $^{\circ}\text{C}$ and 5% CO₂ in growth medium consisting of DMEM with high glucose, 10% FBS, 1 \times pen/strep, 1 \times non-essential amino acids, and appropriate selection antibiotics. At the time of the harvest, the cell density was 80% confluent. One day prior to the assays, cells were harvested by washing with 10 to 20 mL of PBS and treatment with 4 mL of Trypsin solution. After an approximately 5 min incubation at 37 $^{\circ}\text{C}$, the cell suspension was transferred to a 10 mL conical tube and pipette several times to break up cell clusters. After centrifugation, cells were resuspended and prepared in growth medium at a density of 5 \times 10⁵ cell/mL and seeded in 384-well plates for incubation at 37 $^{\circ}\text{C}$ for 16 h in an atmosphere of 5% CO₂. All assays were performed using clear-bottom 384-well plates (Corning, Catalog 3764) on the FLIPR Penta (fluorescence imaging plate reader) from Molecular Devices (Sunnyvale, CA). The FLIPR Calcium 6 Assay Kit (Molecular Devices, catalog R8190) was used for the detection of calcium mobilization upon receptor activation. Prior to the readout, the supernatant was removed from the cells and 20 μL per well of the FLIPR Calcium 6 Assay Kit was added, containing 2 mM probenecid. Plates were incubated with the assay kit for 60 min at 37 $^{\circ}\text{C}$ and 5% CO₂. Kinetics data was acquired by the

FLIPR at the rate of 0.5 Hz. The activity for each individual well activity is interpreted as the difference of the maximum signal after compound addition minus the average baseline fluorescence signal determined before the online addition of compounds. For dose–response experiments, 384-well assay ready serial dilution plates were prepared. The plates contained the five different fractions with 12 different dilution steps (1:3 serial dilution) for each fraction. All samples were diluted in 1× HBSS (Hank's Balanced Salt Solution), 20 mM Hepes, and 0.1% (w/v) BSA. The final compound concentrations in the dose–response experiments ranged from 1.1 μM to 2.1 pM. For concentration–response curves, the following equation was used for the calculations:

$Y = \text{Bottom} + \frac{\text{Top} - \text{Bottom}}{1 + 10^{(\text{Log EC}_{50} - X) \times \text{HillSlope}}}$, where “Y” is a given response, “X” is the log of concentration, “EC₅₀” is the concentration that gives a response half way between Top and Bottom, “HillSlope” describes the steepness of the curve, and “Top” and “Bottom” are plateaus in the units of the Y axis.

In Vitro Affinity Receptor Binding Assay. Membrane preparations from human recombinant HEK-293 cells over-expressing NMUR₂ and [¹²⁵I]NMU-8 were used for the radioligand displacement-binding assay. The specific binding of [¹²⁵I]NMU-8 in the radioligand binding assay was determined with a K_d (dissociation constant) of 0.13 nM.²⁸ When testing the fractions a–e in the competition binding assay, 0.05 nM [¹²⁵I]NMU-8 was used, and nonspecific binding was determined by replacing the radiolabeled NMU-8 with 100 nM unlabeled NMU-8. The incubation time during the various experiments was 60 min at 22 °C using scintillation counting as the detection method. Fractions a–e were tested in 12-point serial dilutions starting from 1 μM to 5.65 pM. Results are expressed as the percentage of control binding

$\left(= \frac{\text{measured specific binding}}{\text{control specific binding}} \times 100 \right)$ and as a percentage inhibition of control specific binding $\left(= 100 - \left[\frac{\text{measured specific binding}}{\text{control specific binding}} \times 100 \right] \right)$, obtained in the presence of the test compounds. The IC₅₀ values (concentration causing a half-maximal inhibition of control specific binding) and Hill coefficients (*n_H*) were determined by the nonlinear regression analysis of the competition curves generated with mean replicate values using Hill equation curve fitting

$Y = D + \frac{A - D}{1 + \left(\frac{C}{C_{50}} \right)^{n_H}}$, where Y is the specific binding, A is the left asymptote of the curve, D is the right asymptote of the curve, C is the compound concentration, C₅₀ refers to IC₅₀, and *n_H* is the slope factor. This analysis was performed using GraphPad Prism software. The inhibition constants (K_i) were calculated using the Cheng–Prusoff equation $K_i = \frac{IC_{50}}{\left(1 + \frac{L}{K_D} \right)}$,

where L is the concentration of the ligand in the assay, and K_D is the affinity of the ligand for the receptor. All radioligand binding experiments were performed at Eurofins Cerep (Celle l'Evescault, France).

Molecular Modeling. Molecular Modeling software: Molecular Operating Environment (MOE), 2022.02; Chemical Computing Group ULC, 1010 Sherbrooke St. West, Suite #910, Montreal, QC, Canada, H3A 2R7, 2022.

³H-Labeling of NMS. A toluene solution of 4 mCi (8 μg, 45 nmol; 1 equiv) [³H]NSP was transferred into a 5 mL LoBind Eppendorf tube. The solvent was removed by a gentle

stream of argon, and the residue was dissolved in 25 μL of DMSO. NMS (713 mg, 188 nmol; 4 equiv), dissolved in 0.5 mL of PBS at pH 8.5, was added to the [³H]NSP solution and shaken horizontally at 250 rpm for 30 min at 22 °C. The solution was put into a 1 mL Float-A-Lyzer for solvent exchange into water. The water was exchanged three times after 30 min and stored in the fridge at 4 °C for 16 h. The crude reaction solution was purified by preparative HPLC to isolate two radioactive peaks that correlate with peaks b and c from the nonradioactive preliminary experiments. Radiochemical purities were >95% for both isolated fractions, with the fraction containing peak b in UV, as in the nonradioactive experiments, consisting of two peaks. The isolated radioactive amount for b was 0.5 mCi and that for c was 0.3 mCi, corresponding to radioactive yields of 13 and 7%, respectively, based on initial 4 mCi. A determination of the molar activity by means of isotope peak patterns from a mass spectrometric analysis was not possible. For this reason, the molar activity of [³H]NSP was taken as 90 Ci/mmol.

AUTHOR INFORMATION

Corresponding Author

Martin R. Edelmann – Department of Pharmacy and Pharmacology, University of Bath, Bath BA2 7AY, U.K.; Roche Pharma Research and Early Development, Roche Innovation Center Basel, Therapeutic Modalities, Small Molecule Research, Isotope Synthesis, F. Hoffmann-La Roche Ltd., CH-4070 Basel, Switzerland; orcid.org/0000-0002-6116-1516; Email: martin.edelmann@roche.com

Authors

Johannes Erny – Roche Pharma Research and Early Development, Roche Innovation Center Basel, Therapeutic Modalities, Small Molecule Research, Lead Discovery, F. Hoffmann-La Roche Ltd., CH-4070 Basel, Switzerland; orcid.org/0000-0002-4166-8803

Wolfgang Guba – Roche Pharma Research and Early Development, Roche Innovation Center Basel, Therapeutic Modalities, Small Molecule Research, Computer Aided Drug Design, F. Hoffmann-La Roche Ltd., CH-4070 Basel, Switzerland; orcid.org/0000-0002-3285-5957

Markus Hierl – Roche Pharma Research and Early Development, Roche Innovation Center Basel, Therapeutic Modalities, Small Molecule Research, Lead Discovery, F. Hoffmann-La Roche Ltd., CH-4070 Basel, Switzerland

Complete contact information is available at:

<https://pubs.acs.org/10.1021/acsomega.2c06758>

Notes

The authors declare the following competing financial interest(s): All authors are in paid employment by the company F. Hoffmann-La Roche AG during the completion of the study.

ACKNOWLEDGMENTS

The authors thank Dr. Ian S. Blagbrough and Prof Stephen M. Husbands (University of Bath, UK) as well as Dr. Michael B. Ottener, Dr. Filippo Sladojevich, and Dr. Dominik Heer (Roche) for their critical proofreading of the manuscript and helpful discussions. We appreciate Prof. William J. S. Lockley (University of Surrey, UK) for scientific discussion on this topic. We thank Raphael Simon Nagorsnik (Roche) for his organizational support.

REFERENCES

- (1) Novak, C. M. Neuromedin S and U. *Endocrinology* **2009**, *150*, 2985–2987.
- (2) Mitchell, J.; Maguire, J.; Davenport, A. Emerging pharmacology and physiology of neuromedin U and the structurally related peptide neuromedin S. *Br. J. Pharmacol.* **2009**, *158*, 87–103.
- (3) Mori, K.; Miyazato, M.; Ida, T.; Murakami, N.; Serino, R.; Ueta, Y.; Kojima, M.; Kangawa, K. Identification of neuromedin S and its possible role in the mammalian circadian oscillator system. *EMBO J.* **2005**, *24*, 325–335.
- (4) Minamino, N.; Kangawa, K.; Matsuo, H. Neuromedin U-8 and U-25: novel uterus stimulating and hypertensive peptides identified in porcine spinal cord. *Biochem. Biophys. Res. Commun.* **1985**, *130*, 1078–1085.
- (5) Wan, Y.; Zhang, J.; Fang, C.; Chen, J.; Li, J.; Li, J.; Wu, C.; Wang, Y. Characterization of neuromedin U (NMU), neuromedin S (NMS) and their receptors (NMUR₁, NMUR₂) in chickens. *Peptides* **2018**, *101*, 69–81.
- (6) Takayama, K.; Mori, K.; Taketa, K.; Taguchi, A.; Yakushiji, F.; Minamino, N.; Miyazato, M.; Kangawa, K.; Hayashi, Y. Discovery of selective hexapeptide agonists to human neuromedin U receptors types 1 and 2. *J. Med. Chem.* **2014**, *57*, 6583–6593.
- (7) Brighton, P. J.; Szekeres, P. G.; Willars, G. B. Neuromedin U and its receptors: structure, function, and physiological roles. *Pharmacol. Rev.* **2004**, *56*, 231–248.
- (8) Tóth, F.; Mallareddy, J. R.; Tourwé, D.; Lipkowski, A. W.; Bujalska-Zadrozny, M.; Benyhe, S.; Ballet, S.; Tóth, G.; Kleczkowska, P. Synthesis and binding characteristics of [³H] neuromedin N, a NTS2 receptor ligand. *Neuropeptides* **2016**, *57*, 15–20.
- (9) De Prins, A.; Martin, C.; Van Wansele, Y.; Skov, L. J.; Tömböly, C.; Tourwé, D.; Caveliers, V.; Van Eeckhaut, A.; Holst, B.; Rosenkilde, M. M.; Smolders, I.; Ballet, S. Development of potent and proteolytically stable human neuromedin U receptor agonists. *Eur. J. Med. Chem.* **2018**, *144*, 887–897.
- (10) Keller, M.; Kuhn, K. K.; Einsiedel, J.; Hübner, H.; Biselli, S.; Mollereau, C.; Wifling, D.; Svobodova, J.; Bernhardt, G.; Cabrele, C.; Vandereyden, P. M. L.; Gmeiner, P.; Buschauer, A. Mimicking of arginine by functionalized N- ω -carbamoylated arginine as a new broadly applicable approach to labeled bioactive peptides: high affinity angiotensin, neuropeptide Y, neuropeptide FF, and neurotensin receptor ligands as examples. *J. Med. Chem.* **2016**, *59*, 1925–1945.
- (11) Yang, H.; Hesk, D. Base metal-catalyzed hydrogen isotope exchange. *J. Labelled Comp. Radiopharm.* **2020**, *63*, 296–307.
- (12) Pfeifer, V.; Certiat, M.; Bouzouita, D.; Palazzolo, A.; Garcia-Argote, S.; Marcon, E.; Buisson, D. A.; Lesot, P.; Maron, L.; Chaudret, B.; Tricard, S.; Rosal, I.; Poteau, R.; Feuillastre, S.; Pieters, G. Hydrogen isotope exchange catalyzed by Ru nanocatalysts: Labelling of complex molecules containing N-heterocycles and reaction mechanism insights. *Chem. – Eur. J.* **2020**, *26*, 4988–4996.
- (13) Loh, Y. Y.; Nagao, K.; Hoover, A. J.; Hesk, D.; Rivera, N. R.; Colletti, S. L.; Davies, I. W.; MacMillan, D. W. C. Photoredox-catalyzed deuteration and tritiation of pharmaceutical compounds. *Science* **2017**, *358*, 1182–1187.
- (14) Valero, M.; Weck, R.; Güssregen, S.; Atzrodt, J.; Derdau, V. Highly selective directed iridium-catalyzed hydrogen isotope exchange reactions of aliphatic amides. *Angew. Chem., Int. Ed.* **2018**, *57*, 8159–8163.
- (15) Zolotarev, Y. A.; Dadayan, A. K.; Bocharov, E. V.; Borisov, Y. A.; Vaskovsky, B. V.; Dorokhova, E. M.; Myasoedov, N. F. New development in the tritium labelling of peptides and proteins using solid catalytic isotopic exchange with spillover-tritium. *Amino Acids* **2003**, *24*, 325–333.
- (16) Wilkes, B. C.; Hruby, V. J.; Yamamura, H. I.; Akiyama, K.; Castrucci, A. M. d. L.; Hadley, M. E.; Andrews, J. R.; Wan, Y.-P. Synthesis of tritium labeled Ac-[Nle⁴, D-Phe⁷]- α -MSH_{4–11}-NH₂: A superpotent melanotropin with prolonged biological activity. *Life Sci.* **1984**, *34*, 977–984.
- (17) Hellio, F.; Lecocq, G.; Morgat, J. L.; Gueguen, P. Total synthesis of fully tritiated leu-enkephalin by enzymatic coupling. *J. Labelled Comp. Radiopharm.* **1990**, *28*, 991–999.
- (18) Pedersen, M. H. F.; Baun, M. Tritium labelling of PACAP-38 using a synthetic diiodinated precursor peptide. *J. Labelled Comp. Radiopharm.* **2012**, *55*, 1–4.
- (19) Shevchenko, V. P.; Nagaev, I. Y.; Myasoedov, N. F. Heterogeneous catalytic synthesis of organic compounds labeled with hydrogen isotopes without using solvents. *Radiochemistry* **2018**, *60*, 105–139.
- (20) Luo, P.; Liu, Z.; Zhang, T.; Wang, X.; Liu, J.; Liu, Y.; Zhou, X.; Chen, Y.; Hou, G.; Dong, W.; Xiao, C.; Jin, Y.; Yang, X.; Wang, F. Photochemical bromination and iodination of peptides and proteins by photoexcitation of aqueous halides. *Chem. Commun.* **2021**, *57*, 11972–11975.
- (21) Schadt, S.; Hauri, S.; Lopes, F.; Edelmann, M. R.; Staack, R. F.; Villaseñor, R.; Kettenberger, H.; Roth, A. B.; Schuler, F.; Richter, W. F.; Funk, C. Are biotransformation studies of therapeutic proteins needed? Scientific considerations and technical challenges. *Drug Metab. Dispos.* **2019**, *47*, 1443–1456.
- (22) Edelmann, M. R.; Kettenberger, H.; Knaupp, A.; Schlothauer, T.; Otteneder, M. B. Radiolabeled IgG antibodies: Impact of various labels on neonatal Fc receptor binding. *J. Labelled Comp. Radiopharm.* **2019**, *62*, 751–757.
- (23) Wang, M.; Zhan, Y.; O’Neil, S. P.; Harris, S.; Henson, C.; McEwen, A.; Webster, R.; O’Hara, D. M. Quantitative biodistribution of biotherapeutics at whole body, organ and cellular levels by autoradiography. *Bioanalysis* **2018**, *10*, 1487–1500.
- (24) Kumar, K.; Woolum, K. A novel reagent for radioiodine labeling of new chemical entities (NCEs) and biomolecules. *Molecules* **2021**, *26*, 4344.
- (25) Peng, C. T.; Hua, R. L.; Souers, P. C.; Coronado, P. R. Tritium labeling of amino acids and peptides with liquid and solid tritium. *Fusion Technol.* **1988**, *14*, 833–839.
- (26) Tóth, G.; Lovas, S.; Ötvös, F. (1997) Tritium Labeling of Neuropeptides, in *Neuropeptide Protocols*; (Irvine, G. B., Williams, C. H., Eds.) pp. 219–230, Humana Press: Totowa, NJ.
- (27) Roepstorff, P.; Fohlman, J. Letter to the editors. *Biomed. Mass Spectrom.* **1984**, *11*, 601.
- (28) Funes, S.; Hedrick, J. A.; Yang, S.; Shan, L.; Bayne, M.; Monsma, F. J., Jr.; Gustafson, E. L. Cloning and characterization of murine neuromedin U receptors. *Peptides* **2002**, *23*, 1607–1615.
- (29) You, C.; Zhang, Y.; Xu, P.; Huang, S.; Yin, W.; Eric Xu, H.; Jiang, Y. Structural insights into the peptide selectivity and activation of human neuromedin U receptors. *Nat. Commun.* **2022**, *13*, 2045.